

# Speciation of Linear and Branched Hydrocarbons by a Fluorinated Polyimide Film-Based Surface Acoustic Wave Sensor

Andrea E. Hoyt and Antonio J. Ricco\*

Microsensor Research and Development Department  
Sandia National Laboratories  
Albuquerque, New Mexico 87185-1425

Huey C. Yang and Richard M. Crooks\*

Department of Chemistry, Texas A&M University  
College Station, Texas 77843-3255

Received April 6, 1995

We report a surface acoustic wave (SAW) device-based sensor that uses a fluorinated polyimide film as the chemically sensitive interface to preferentially detect linear over branched alkane isomers. Linear hydrocarbons penetrate the film, producing a change in mass that is over 100 times larger than for comparable concentrations of the branched isomer of the same alkane, consistent with very limited penetration by the latter. Results were confirmed using real-time FTIR external-reflection spectroscopy (ERS), which also shows that the penetration of normal alkanes results in conformational changes to the polymer; no similar effects are observed as a result of exposure to branched alkanes.

The polyimide was synthesized from 2,2'-bis(trifluoromethyl)-4,4'-diaminobiphenyl (TFMB, Marshallton) and 4,4'-[2,2,2-trifluoro-1-(trifluoromethyl)ethylidene]bis[1,3-isobenzofurandione] (6FDA, Hoechst-Celanese) using the high-temperature process described by Harris.<sup>1</sup> Phthalic anhydride (Aldrich) was used for molecular weight control and to afford nonreactive end groups. The reaction and resulting repeat unit are shown in Scheme 1. The polyimide was dissolved in chloroform and spin cast to yield 300-nm-thick films on the entire surface of 97-MHz ST-quartz SAW delay lines, or onto Au-coated Si substrates for IR studies. Description of SAW device design and fabrication, drive circuitry, data collection methods, and gas flow system can be found elsewhere.<sup>2,3</sup> For vapor exposures, coated SAW devices were allowed to stabilize in flowing (1.0 L/min) ultrahigh-purity N<sub>2</sub> and then were exposed to a N<sub>2</sub> stream with entrained hydrocarbon solvent vapor. SAW response is reported in parts per million (ppm) frequency shift (1 ppm  $\approx$  97 Hz  $\approx$  7.7 ng/cm<sup>2</sup> mass change). The device and fixture were maintained at 20.00  $\pm$  0.03 °C. Details of the *in-situ* FTIR-ERS instrumentation, including custom vapor-phase flow cell, are reported elsewhere.<sup>4</sup> FTIR-ERS spectra, each consisting of 64 individual scans (4 cm<sup>-1</sup> resolution), were collected every 1.5 min during each experiment.

The response of a polymer-coated SAW device to vapor-phase analytes depends upon many parameters. Sorption-related increases in film mass lead to decreases in wave velocity, and hence oscillation frequency. Changes in the viscoelastic properties of the film also affect the wave velocity, as well as amplitude.<sup>5</sup> Other parameters such as film electrical conductivity and permittivity can affect both SAW velocity and amplitude, but only for ranges of these parameters that do not apply to the experiments described here. It is important to note that

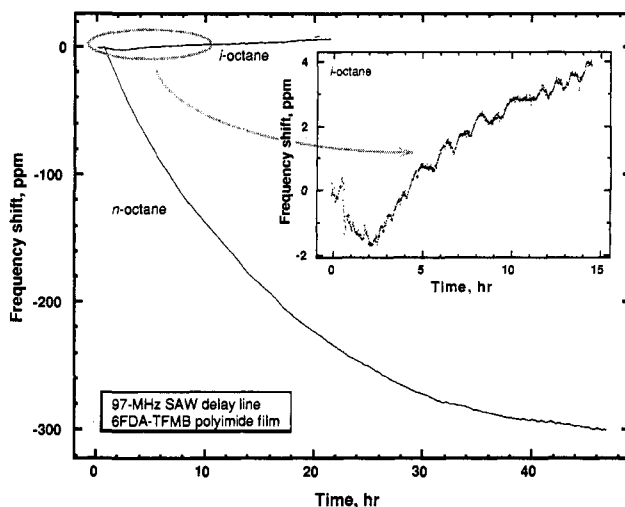
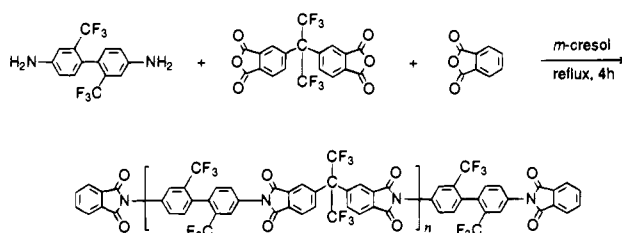


**Figure 1.** Frequency shifts vs time for 6FDA-TFMB-coated 97-MHz SAW device upon exposure to *n*-octane (30% of saturation vapor pressure) and isooctane (50% of saturation vapor pressure), showing the exceptional permselectivity of this film for linear vs branched hydrocarbons. Inset is an expanded view of the isooctane response, showing that mass-loading effects during the first 2.5 h (corresponding to just  $1 \times 10^{-10}$  mol/cm<sup>2</sup> of isooctane) are eventually overbalanced by antiplasticization (stiffening) of the film by the absorbed solvent. Any such stiffening in the case of *n*-octane is small compared to the mass-loading signal from solvent absorption.

## Scheme 1



acoustically thin polymer films must be used in order to interpret SAW response solely in terms of mass loading.<sup>6</sup> An elastic film, generally including metals, ceramics, and many glassy polymers, is considered acoustically thin<sup>6</sup> if its thickness  $h \ll \Lambda_0(v_f/v_0)^2$ , where  $\Lambda_0$  and  $v_0$  are the respective SAW wavelength and velocity in the substrate, and  $v_f$  is the acoustic shear-wave velocity in the film (derivation based on ref 5). If  $h$  is no more than 1–3% of the product  $\Lambda_0(v_f/v_0)^2$ , the film is likely to behave as “acoustically thin”; the films used in this work meet this criterion. A detailed discussion of acoustically thick vs thin films can be found in a recent paper by Martin *et al.*<sup>5</sup>

The frequency shifts recorded as a function of time upon exposure of a 6FDA-TFMB-coated SAW device to *n*-octane and isooctane are shown in Figure 1; the vapor concentration was 30% of saturation for *n*-octane and 50% for isooctane. The response to *n*-octane is about -300 ppm at equilibrium; for isooctane, the response is +6 ppm after 20 h of exposure. The inset to Figure 1 shows that a frequency shift of -1.5 ppm occurred during the first 2.5 h of film exposure to isooctane. We interpret this initial shift (corresponding to just  $1 \times 10^{-10}$  mol/cm<sup>2</sup> of isooctane) to be a result of mass loading of the film by surface-adsorbed isooctane, plus a very small amount of dissolved isooctane. With longer exposure, the isooctane has a minor antiplasticizing effect on the film, with the resultant increase in polymer stiffness causing a small, positive frequency shift that overbalances the mass loading. While minor stiffening may also occur during *n*-octane exposure, any such effect is small compared to mass loading due to absorbed vapor.

(6) Ricco, A. J. *Electrochem. Soc. Interface* 1994, 3, 38–44.

\* Authors to whom correspondence is to be addressed.

(1) Harris, F. W.; Hsu, S. L. C. *High Perform. Polym.* 1989, 1, 3–16.

(2) Ricco, A. J.; Martin, S. J. *Thin Solid Films* 1991, 206, 94–101.

(3) Frye, G. C.; Martin, S. J.; Ricco, A. J. *Sens. Mater.* 1989, 1, 335–57.

(4) Xu, C.; Sun, L.; Kepley, L. J.; Crooks, R. M.; Ricco, A. J. *Anal. Chem.* 1993, 65, 2102–7.

(5) Martin S. J.; Frye, G. C.; Senturia, S. D. *Anal. Chem.* 1994, 66, 2201–19.

The phenomenon (at constant temperature) of antiplasticization at low diluent (absorbate) concentrations, which often changes over to plasticization at high concentrations of the same diluent, has been observed for many diluent/polymer systems.<sup>7-9</sup> Low-concentration antiplasticization is most frequently attributed to filling of excess free volume in a glassy polymer,<sup>8</sup> this phenomenon eventually being overwhelmed as diluent concentration increases: addition of sufficient low-molecular-weight diluent to the polymer diminishes its modulus.<sup>10</sup> In the present instance, we believe that the isooctane does indeed fill free volume in the polymer, but its dissolved concentration cannot attain a high enough level for plasticization to occur. In the case of *n*-octane, the much higher concentration immediately absorbed by the film and the resultant response of the SAW device to mass loading mask any modulus effects.

The linear/branched discriminatory effect is not unique to the octane isomers. The response to *n*-hexane,  $-375$  ppm, is about 150 times larger than that of isohexane, with both vapors at 30% of saturation.

The total mass/area of the 300-nm-thick polymer film is about  $30 \mu\text{g}/\text{cm}^2$ ; the response to *n*-hexane is consistent with absorption of a total mass/area of  $2.7 \mu\text{g}/\text{cm}^2$  of this alkane, a significant 9% by weight of the host matrix; for *n*-octane, the loading exceeds 7% by weight. In contrast, the mass loading part of the responses to isohexane and isooctane corresponds to less than 0.1% of the mass of the 6FDA-TFMB polyimide film.

SAW results were confirmed by *in-situ* FTIR-ERS. Film-coated substrates were exposed to a pure  $\text{N}_2$  stream for 10 min and then to analyte (*n*-hexane, isooctane) vapor streams for 18 min. During dosing, the spectra of gaseous *n*-hexane and isooctane in the flow cell dominate. The difference between linear and branched analytes is most apparent when the flow cell has been purged of hydrocarbon vapor for 2 min. As shown in Figure 2 (lower spectrum), C-H stretching features due to polymer-dissolved *n*-hexane (cluster of peaks near  $2900 \text{ cm}^{-1}$ ) are clearly evident, as is a fairly large (positive) peak at  $1466 \text{ cm}^{-1}$ , likely a hexane C-H bending vibration. The corresponding spectrum for isooctane (top) is featureless; each spectrum uses the undosed polymer film as a (subtractive) reference.

During and after purging away the *n*-hexane with dry  $\text{N}_2$ , significant negative absorbances remain in the region below  $2000 \text{ cm}^{-1}$  (Figure 2); no similar features appear in the isooctane spectrum. These negative absorbances, which probably result from a dissolved-hexane-induced change in the optical properties of the polymer film,<sup>11</sup> correspond precisely with bands characteristic of the virgin polymer. We believe that the absorption of hexane increases the density of the polymer film and hence its index of refraction, causing a decrease in the angle of incidence at the gold surface, which in turn causes a decrease in the standing electric field at the polymer/metal interface, the ultimate effect of which is to diminish the intensity of the polymer's infrared absorbances.<sup>11</sup> The most obviously affected polymer bands include imide C=O stretching modes ( $1793 \text{ cm}^{-1}$ ,  $1747 \text{ cm}^{-1}$ ), aromatic C=CC stretch ( $1495 \text{ cm}^{-1}$ ), aromatic C-H bend ( $1430 \text{ cm}^{-1}$ ), and the C-N stretch ( $1379 \text{ cm}^{-1}$ ).

Our SAW and FTIR results are consistent with shape/size selectivity, with the more spherical branched hydrocarbons being excluded and the more "worm-like" linear hydrocarbons penetrating the film; the penetration mechanism may be analogous

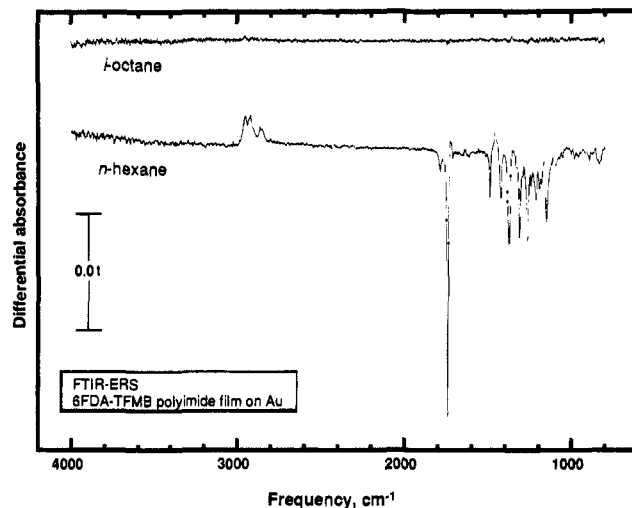


**Figure 2.** *In-situ* FTIR-ERS difference spectra for 6FDA-TFMB-coated Au-on-Si substrates obtained 2 min after the flow of vapor-phase analyte was replaced by a pure  $\text{N}_2$  purge. Top: isooctane. Bottom: *n*-hexane. The spectrum of the undosed polymer film serves as reference in both cases. The top spectrum shows no detectable evidence of isooctane, but the bottom spectrum shows (positive) C-H stretching and bending bands due to polymer-dissolved *n*-hexane, as well as a number of (negative) bands associated with the polyimide, indicating changes in polymer optical properties that result from the presence of the *n*-hexane solvent.

to the reptation model of polymer diffusion.<sup>12</sup> Similar selectivity trends are also the basis of cross-linked polystyrene stationary-phase columns utilized in size-exclusion chromatography (SEC), with two significant differences. First, the selectivity of the 6FDA-TFMB polyimide film for penetration of linear hydrocarbons depends strongly on geometry, rather than overall molecular size (in the sense of molar volume); second, separation is effected by the equivalent of *only a single theoretical plate*. In contrast, the resins used in SEC columns exhibit their size-exclusion abilities over an extremely large number of theoretical plates. Arguably the closest analogy to the selectivity we observe is the well-known size/shape selectivity of zeolitic materials, the pores of which are impervious to molecules with critical dimensions larger than the crystalline pore diameter.

In summary, we have demonstrated effective discrimination between linear and branched hydrocarbons using a polymer-coated SAW sensor. We believe that the speciation results because the chains of this polymer pack together unusually closely and uniformly, with access to the interconnected "free volume" of the polymer film being through openings large enough to pass methyl or methylene groups, but too small for a CH-CH<sub>3</sub> unit to go through "sideways". The range of hydrocarbons to which this effect extends, the dependence of separation efficiency on film preparation techniques, and models of polymer chain packing to explain these results are under investigation.

**Acknowledgment.** The authors are grateful to Mark Hill and Mary-Anne Mitchell of Sandia National Laboratories (SNL) for their expert technical assistance. Work at SNL was performed under the auspices of the U.S. Department of Energy, Contract No. DE-AC04-94AL85000. Work at Texas A&M University is supported by contract from SNL and by the National Science Foundation (CHE9313441).

JA951118W

(7) Jackson, W. J.; Caldwell, J. R. *J. Appl. Polym. Sci.* **1967**, *11*, 211-226.

(8) Maeda, Y.; Paul, D. R. *J. Membr. Sci.* **1987**, *30*, 1-9.

(9) Petrie, S. E. B.; Moore, R. S.; Flick, J. R. *J. Appl. Phys.* **1972**, *43*, 4318-26.

(10) Aklonis, J. J.; MacKnight, W. J. *Introduction to Polymer Viscoelasticity*, 2nd ed.; Wiley Interscience: New York, 1983; pp 43-4.

(11) Porter, M. D. *Anal. Chem.* **1988**, *60*, 1143A-55A.

(12) deGennes, P. G. *J. Chem. Phys.* **1971**, *55*, 572-9.